Nationaal Lucht- en Ruimtevaartlaboratorium
National Aerospace Laboratory NLR

Executive summary

Teardown of a GLARE window area from the Airbus MegaLiner Barrel fatigue test article

Problem area
NDI and teardown fractography of a GLARE window panel (F4) from the Airbus MegaLiner Barrel (MLB) fatigue test.

Description
Fractography was used to verify NDI results and determine fatigue crack growth behaviour of GLARE skin and window frame cracks.

Results and conclusions
Fractography demonstrated that the NLR's teardown NDI capability is excellent. The MLB load spectrum marked the fatigue fracture surfaces. This made it possible to trace crack growth back from the end of the test, notably for the window frame material (7175-T73 aluminium alloy). Tracing crack growth was much more difficult for the GLARE aluminium layers (2024-T3 alloy). The largest traceable GLARE aluminium crack grew significantly slower than the largest window frame crack. All the GLARE aluminium cracks were less than 1mm in size, demonstrating the excellent fatigue damage tolerance capability of the GLARE skin.

Report no.
NLR-TP-2006-183

Author(s)
R.J.H. Wanhill
D.J. Platenkamp
T. Hattenberg
A.F. Bosch

Classification report
Unclassified

Date
April 2006

Knowledge area(s)
Vliegtuigmateriaal- en schadeonderzoek

Descriptor(s)
fatigue
non-destructive inspection
fibre-metal laminates
GLARE

This report is based on a presentation held at SIF 2006, Sydney, September 2006.

Teardown of a GLARE window area from the Airbus MegaLiner Barrel fatigue test article

Nationaal Lucht- en Ruimtevaartlaboratorium, National Aerospace Laboratory NLR

Anthony Fokkerweg 2, 1059 CM Amsterdam,
P.O. Box 90502, 1006 BM Amsterdam, The Netherlands
Telephone +31 20 511 31 13, Fax +31 20 511 32 10, Web site: www.nlr.nl

Nationaal Lucht- en Ruimtevaartlaboratorium
National Aerospace Laboratory NLR

NLR-TP-2006-183

Teardown of a GLARE window area from the Airbus MegaLiner Barrel fatigue test article

R.J.H. Wanhill, D.J. Platenkamp, T. Hattenberg and A.F. Bosch

This report is based on a presentation held at SIF 2006, Sydney, September 2006.

This publication has been refereed by the Advisory Committee AEROSPACE VEHICLES.

Customer	National Aerospace Laboratory NLR
Contract number	----
Owner	National Aerospace Laboratory NLR
Division	Aerospace Vehicles
Distribution	Unlimited
Classification of title	Unclassified
	September 2007

Author	Reviewer	Managing department

Summary

The MegaLiner Barrel (MLB) test was done to study the fatigue behaviour of a double-deck fuselage configuration. The test was part of the Airbus 380 development programme, and was discontinued after 45,402 simulated flights. The NLR is carrying out teardowns and supplemental fatigue tests of GLARE (GLAss REinforced aluminium laminate) panels from several key locations of the MLB. This paper describes the teardown of a GLARE window area. The teardown began with Non-Destructive Inspection (NDI), and was followed by fractographic investigation of the NDI-indicated cracks. The teardown had the following main objectives, which were largely achieved:

- verification of NDI techniques and capabilities
- establishing the patterns of cracking in the GLARE aluminium layers
- determination of fatigue initiation locations and likely causes
- estimation of fatigue "initiation" lives and crack growth behaviour in the GLARE aluminium layers
- provision of data to verify and possibly improve current fatigue crack growth models for GLARE.

Contents

1 Introduction 9

2 The GLARE window area 10

3 Teardown checklist 11

4 MLB fatigue load spectrum 12

5 NDI practical details 13

5.1 Window area disassembly 13

5.2 NDI inspection details and verification 13

6 NDI results 15

6.1 C-scan inspections 15

6.2 Eddy current inspections 15

7 NDI verification and analysis 16

7.1 Verification of NDI crack indications 16

7.2 Statistical analysis of GLARE cracks 17

7.3 Patterns of cracking in the GLARE skin 18

7.4 Comparison of GLARE skin and window frame cracks at the same fastener holes 19

7.5 Fatigue initiation locations in the GLARE skin 19

8 Fractography 20

8.1 Background information 20

8.2 Detailed objectives 20

8.3 Practical details 20

8.4 Fractographic “readability” of the MLB fatigue load spectrum 21

8.5 Fractographic analysis of the largest window frame crack 21

8.6 Fractographic analysis of the GLARE cracks 22

9 Concluding discussion **23**

9.1 NDI verification 23

9.2 Low-magnification fractography 23

9.3 Detailed fractography 23

9.4 Verification of GLARE crack growth models 24

References **25**

7 Tables

11 Figures

This page is intentionally left blank.

1 Introduction

The pressure cabin MegaLiner Barrel (MLB) test was initiated by Airbus Deutschland in the mid-1990s to study the fatigue behaviour of a double-deck fuselage configuration. Several design solutions, structural materials and joining methods were investigated, and the applied fatigue load spectrum was set at a level high enough to obtain fatigue damage. The results contributed to the subsequent robust design of the Airbus A380.

The test was done in Hamburg, Germany, and was discontinued after 45,402 simulated flights. Stork/Fokker Aerospace then specified a programme of teardown and additional fatigue testing for GLARE (GLAss REinforced aluminium laminate) panels from several key locations of the MLB. This programme is being done by the NLR.

This paper describes the teardown of a GLARE window area. Stork/Fokker chose this window area because it included artificial damage, a 6mm diameter Teflon foil insert, in the GLARE skin near a window cutout. Also, Airbus Hamburg requested investigation of fatigue cracking at fastener holes.

The teardown began with Non-Destructive Inspection (NDI), followed by fractographic investigation of the NDI-indicated cracks. The main objectives were:

1) Verification of NDI techniques and capabilities.
2) Establishing the patterns of cracking in the GLARE aluminium layers.
3) Determination of fatigue initiation locations and likely causes.
4) Estimation of fatigue “initiation” lives and crack growth behaviour in the GLARE aluminium layers.
5) Provision of data to verify and possibly improve fatigue crack growth models for GLARE.

2 The GLARE window area

Figure 1 shows the GLARE window area shortly after its removal from the MLB. The window area has two identical windows, which are the A340 shape rather than the A380 elliptical shape. This difference is unimportant for the present work.

The basic structure of the window area is a GLARE 3-7/6-0.3/0.4 skin fastened to die forged 7175-T73 aluminium alloy window frames by press fit 3/16" (4.76mm) Hi-Loks. The GLARE code means seven 2024-T3 aluminium alloy layers 0.3mm or 0.4mm thick interleaved with six glass fibre layers. In fact, the outer two aluminium layers were 0.4mm thick and the inner five layers were 0.3mm thick.

3 Teardown checklist

The teardown checklist is given in table 1. This includes partial teardown NDI

Table 1 Teardown checklist

Partial teardown (NDI)

- Fastener removal around windows, followed by eddy current rotor inspection of fastener hole bores.

Teardown I (NDI)

- Removal of aluminium window frames using plastic wedges to carefully disbond the faying surface sealant.
- Ultrasonic (C-scan) NDI to find and check the artificial damage (Teflon foil insert).
- Eddy current pencil probe inspection of GLARE and aluminium window frame fastener holes on the faying surface sides.
- Disassembly of window frames and eddy current pencil probe inspection of the aluminium rebates.

Teardown II (fractography)

- All NDI-indicated cracked fastener holes in GLARE skin removed from both windows and forcibly opened.
- Low-magnification (optical) fractography to verify and map fatigue cracks in the aluminium layers of the opened-up GLARE fastener holes.
- All aluminium window frame fastener holes underlying the NDI-indicated cracked fastener holes in GLARE skin removed and forcibly opened.
- Low-magnification (optical) fractography to verify and map fatigue cracks in the aluminium window frame fastener holes.

Teardown III (fractography)

- FEG-SEM fractography of largest fatigue crack in either of the aluminium window frames, looking for fatigue striations and crack growth markings due to MLB spectrum peak loads.
- Verification of MLB spectrum "readability", whereby fatigue crack growth can be traced back to small crack sizes.

Teardown IV (fractography)

- Selection of two GLARE fatigue fracture surfaces:
  (1) containing the largest fatigue crack in any aluminium layer,
  (2) the fatigue fracture surface at the same position as the largest fatigue crack in either of the aluminium
  window frames.
- Preparation of the selected GLARE fatigue fracture surfaces for FEG-SEM fractography. This requires disassembly of the GLARE, using a low-temperature oxygen plasma treatment to degrade the adhesive layers.
- FEG-SEM fractography of the largest fatigue cracks in the aluminium layers of the two disassembled GLARE fatigue fracture surfaces, looking for fatigue striations and crack growth markings due to MLB spectrum peak loads. For (2) above this turned out to be impractical, see subsection **8.6**.
- Verification of MLB spectrum "readability", whereby fatigue crack growth can be traced back to small crack sizes.

4 MLB fatigue load spectrum

The MLB fatigue load test spectrum was defined by Wagner (2001) [1]. The spectrum is based on a 6.25 hour mission, and includes basic ground and flight loads, with incremental loads for taxiing, rotation, landing, vertical and lateral gusts, and coordinated turns. There are eight basic flight types, ranging from severe turbulence (A) to calm air (H). Flight type A is combined with one ground load condition (Z); type B with two ground load conditions (Y, Z); and types C – H with three ground load conditions (X, Y, Z), resulting in a total of 21 flight types. These 21 flight types occur with differing frequencies in a block of 2150 flights, which is then repeated until the end of testing.

The spectrum is complex in detail, but for the present purpose it can be regarded simply in terms of the maximum load in the window area during each simulated flight. The maximum loads represent internal pressure + shear loads that are mainly due to the maximum vertical gust loads in each flight.

Table 2 gives the positions of only the severest flight types A − C in each flight block. The fractographic analyses in subsections **8.4** – **8.6** relied almost entirely on crack front markings due to these flight types.

Table 2 Severest flights in the MLB load spectrum

A	**B**	**C**
1379	58,127, 196,1094	139,148,366,494,671,956,1026, 1392,1549,1785,1854,1928

5 NDI practical details

5.1 Window area disassembly

The Hi-Lok fasteners were carefully removed for the first eddy current inspections and C-scan mapping. Then the aluminium window frames needed to be separated from the GLARE skin. This was done by using small plastic wedges carefully driven between the aluminium window frames and the GLARE skin. Figure 2 illustrates the fully disassembled parts.

The reasons for disassembly are:

- C-scan inspection in the (partially) assembled condition would have been affected by transmission of ultrasound into the aluminium window frame. When only the GLARE skin is inspected a clear rear wall reflection is obtained without disturbing influences from the back-up structure.
- Prevention of disturbing interface signals between the aluminium window frames and the GLARE skin during the second eddy current rotor inspections.
- Providing access to the faying surfaces of the GLARE skin, the aluminium window frames, and the rebates in order to do eddy current pencil probe inspections.

5.2 NDI inspection details and verification

Ultrasonic inspection

C-scans were done in an immersion tank, type AI 1512-S2-T. The Harisonic 14-0110-S immersion transducer had a diameter of 0.625", a focus distance of 1", and operated at 1 MHz.

The ultrasonic flaw detector was a Krautkrämer USIP−40. The data acquisition and analysis system was from Ultrasonic Sciences Ltd.

A GLARE 3-10/9-0.4 reference specimen containing nine Flat Bottom Holes (FBHs) was used to calibrate the set-up. The FBHs were depth-drilled to represent delaminations between each pair of aluminium and glass fibre layers.

Eddy current rotor inspection

Fastener hole inspection was done with a Nortec 2000 instrument from Stavely NDT Technologies and a hand-held differential shielded rotor probe of the spring-loaded expandable type. The probe was 3/16" in diameter and operated at 500 kHz and 1000 – 1500 RPM.
An expandable probe has the advantage of less critical vertical alignment. It also compensates for any small variations in hole diameter.

Eddy current inspection of hole countersinks

Figure 3 shows several fatigue initiation possibilities in the GLARE aluminium layers. The "intermediate" and "non-knife edge" types can be detected with a cylindrical rotor probe. Fatigue cracks that initiate at "knife edges" require special countersink probes: otherwise, the countersink inspections follow the same procedure as the rotor probe inspections. The countersink probe was 3/16" in diameter and operated at 300 kHz and 1000 – 1500 RPM.

Eddy current pencil probe inspection

Pencil probe inspection checked for cracks at the faying surfaces of the GLARE skin and aluminium window frames, and also any cracks in the aluminium rebates. The probe was of the surface reflection type with a shielded absolute coil and was not directionally sensitive. The coil diameter was about 1mm, and the probe operated between 300 kHz and 1 MHz.

NDI verification: opening up cracks

Figure 4 shows the procedure for opening up cracks in GLARE. NDI-indicated fastener holes are removed with a jeweller's saw. These are sectioned through the holes, v-notched, and obliquely cut into (if there are uncracked aluminium layers) before bending to failure. In this way the glass fibre resistance to fracture can be minimised and there is less risk of distorting the aluminium layers. The same procedure was used for the aluminium window frames.

6 NDI results

6.1 C-scan inspections

The GLARE skin was C-scanned around the window cutouts. The 6mm diameter Teflon foil insert was readily detected by both attenuation and reflection measurements, for example figure 5. The measurements showed that the MLB fatigue test did not cause delamination growth from the insert.

6.2 Eddy current inspections

Eddy current rotor inspections

53 crack indications were obtained for the fastener hole bores in the partially assembled condition, and 49 indications in the fully disassembled condition. The crack indications were almost equally divided between the windows: figure 6 shows 19 and 22 indications for the GLARE skin around windows C64 – C65 and C65 – C66 respectively; and 5 and 3 indications for the corresponding aluminium alloy window frames.

Figure 6 also shows that most of the crack indications were in the **B** and **D** quadrants. These were the quadrants largely subjected to tensile shear loads during the MLB fatigue test.

Eddy current inspection of hole countersinks

Only two crack indications were obtained for the fastener hole countersinks in the GLARE skin: one at hole B6 for window C64 – C65, and the other at hole B4 for window C65 – C66 (see figure 6 for the hole locations). These indications were not confirmed by a pencil probe check, so any cracks would have to have been small: see subsection **7.3**.

Eddy current pencil probe inspections

The pencil probe inspections of the GLARE skin and aluminium window frames were done because fatigue cracks often initiate from faying surface fretting. However, only 11 crack indications were obtained, see table 3, and visual examination of the faying surfaces showed no evidence of fretting, probably because of the faying surface sealant used during assembly.

Table 3 Pencil probe crack indications for the GLARE skin and aluminium window frames

Window	Component	Fastener hole
C64 – C65	GLARE skin aluminium frame	B13,B14 B18,B26,D17
C65 – C66	GLARE skin aluminium frame	B4,C14,D6,D14 B26,D19

Finally, no crack indications were found for the aluminium rebates, although visual examination showed some fretting near the fastener holes.

7 NDI verification and analysis

7.1 Verification of NDI crack indications

Table 4 lists the overall results of opening up the NDI-indicated fastener holes in the GLARE skin. Low-magnification fractography verified the NDI crack indications for all fastener holes with maximum crack lengths $a_{max} \geq 0.24$mm.

Table 4 Verification of NDI for the GLARE skin

Window area C64 – C65		
Fastener hole	**a_{max} (mm)**	**NDI + fractography result**
A15	–	false call
B1	0.27	**v**
B2	0.14	not detected by NDI
B3	0.35	**v**
B4	0.23	not detected by NDI
B5	0.43	**v**
B6	0.56	**v**
B13	0.53	**v**
B14	0.57	**v**
B18	0.10	not detected by NDI
B22	0.26	**v**
B23	0.49	**v**
C15	–	false call
D2	0.14	not detected by NDI
D3	0.37	**v**
D4	0.16	**v**
D5	0.46	**v**
D16	0.11	not detected by NDI
D17	0.33	**v**
D19	0.17	not detected by NDI
A14	0.20	**v**
A15	–	false call
B2	0.50	**v**
B3	0.57	**v**
B4	0.95	**v**
B5	0.57	**v**
B6	0.17	not detected by NDI
B7	0.46	**v**
C14	0.54	**v**
C15	–	false call
D2	0.57	**v**
D3	0.33	**v**
D4	0.36	**v**
D5	0.12	not detected by NDI
D6	0.43	**v**
D14	0.30	**v**

Window area C64 – C65		
Fastener hole	**a_{max} (mm)**	**NDI + fractography result**
D16	0.12	not detected by NDI
D17	0.24	**v**
D18	0.29	**v**
D19	0.42	**v**

v: verified crack indication

Note that the false calls came from fastener holes on the long axes of the windows (see figure 6). A likely explanation is that these holes were used as locators for attaching the aluminium window frames to the GLARE skin, and that this locator function led to hole damage sufficient to cause the NDI indications.

Table 5 gives the results of opening up the NDI-indicated fastener holes in the aluminium window frames. Fractography showed there was one false call, at the same C15 fastener hole as a false call for the GLARE skin, see the first part of table 4. This additional false call supports the likelihood of hole damage mentioned above.

Table 5 Verification of NDI for the aluminium window frames

Window area C64 – C65		
Fastener hole	**a_{max} (mm)**	**NDI + fractography result**
B18	0.52	**v**
B26	1.36	**v**
C15	–	false call
D16	0.36	**v**
D17	0.91	**v**
Window area C65 – C66		
Fastener hole	**a_{max} (mm)**	**NDI + fractography result**
B26	0.69	**v**
D2	0.35	**v**
D19	1.68	**v**

v: verified crack indication

7.2 Statistical analysis of GLARE cracks

The NDI and low-magnification fractography results for the GLARE skin provide possibilities for statistical analysis using the following results:

- A "hit" is when a crack existed and NDI detected it.

- A "miss" is when a crack existed but NDI did not detect it.
- A "false call" is when a crack did not exist but NDI indicated it.

A Probability Of Detection (POD) curve can be obtained from the hit/miss data, provided the number of false calls is no more than 5% of the total number of inspections (Vukelich *et al*. 1993) [2]. From table 4 and figure 6 it is seen that there were 4 false calls for a total number of 216 inspected fastener holes. The false call rate was thus less than 2%.

A POD curve represents the chances of detecting cracks of different lengths. The most appropriate distribution function for this curve is the log-normal function (Fahr *et al*. 1993 [3]; Vukelich *et al*. 1993 [2]). On this basis the POD computation for the data in table 4 was done by Grooteman (2005) [4].

Figure 7 shows the mean (50% confidence) POD curve. For the often used 90% probability + 50% confidence level the detectable crack length is 0.25mm. This is an excellent result, owing to few misses and the relatively small sizes of the missed cracks: note that in subsection **7.1** it was stated that fractography verified the NDI crack indications for all fastener holes with maximum crack lengths ≥ 0.24mm.

In practical terms this result shows that the NLR's teardown NDI capability is excellent, and that most cracks in GLARE will be detected during teardown.

7.3 Patterns of cracking in the GLARE skin

Figure 8 gives examples of the cracking patterns in the aluminium layers of the GLARE skin. Most cracks were in the fastener hole bores. Only a few cracks grew from the countersinks, and then only in layer 3. The largest countersink crack is shown in figure 8: this had a length of 0.42mm.

Table 6 lists the layer positions of the largest cracks on both sides of each fastener hole. Most were in layer 5, like three of the four examples in figure 8.

Table 6 Positions of largest cracks in GLARE skin

Aluminium layer						
1	2	3	4	5	6	7
0	0	0	8	21	8	14

The smaller cracks in figure 8 show that they began from one or both corners of an aluminium layer. This was also the case for all the other cracked fastener holes in the GLARE skin.

7.4 Comparison of GLARE skin and window frame cracks at the same fastener holes

Table 7 compares the maximum crack lengths for the same fastener holes in the GLARE skin and aluminium window frames. The window frame a_{max} values were generally significantly larger, implying that they would be more easily detected in both the partially and fully disassembled conditions.

Table 7 GLARE and window frame cracks at the same fastener holes

Window area C64 – C65		
Fastener hole	**GLARE a_{max} (mm)**	**Window frame a_{max} (mm)**
B18	0.10	0.52
B26	–	1.36
D16	0.11	0.36
D17	0.33	0.91
Window area C65 – C66		
Fastener hole	**GLARE a_{max} (mm)**	Window frame **a_{max} (mm)**
B26	–	0.69
D2	0.57	0.35
D19	0.42	1.68

7.5 Fatigue initiation locations in the GLARE skin

The patterns of cracking in the GLARE skin, illustrated in figure 8, showed that the smaller cracks (and presumably the larger ones also) all began at the corners of the aluminium layers. Thus the most likely causes of fatigue crack initiation, besides the severity of the applied MLB fatigue load spectrum, are the stress concentrations provided by these corners.

On the other hand, this does not explain why many more cracks began in the fastener hole bores (layers 4 – 7) rather than in the countersinks (layers 1 – 3), where there are so-called “knife edges”. It is possible that local secondary bending favoured fatigue initiation in the fastener hole bores. Support for this hypothesis comes from the window frame cracks. These were all corner cracks with maximum depths along the fastener hole bores larger than a_{max} .

8 Fractography

8.1 Background information

Detailed fractography of fatigue damage in aircraft structures is time-consuming and requires much expertise. For these reasons it is seldom done. However, the knowledge gained is essential to understanding how fatigue damage really happens and accumulates, *as opposed to what may be assumed*: see, for example, an investigation of conventional pressure cabin lap splices by Wanhill *et al*. (2001) [5].

Until now there have been no detailed fractographic analyses of fatigue damage in full-scale GLARE structural components. The MLB test provided a unique opportunity to attempt such analyses.

8.2 Detailed objectives

- Use the largest crack in either of the aluminium window frames to verify the fractographic "readability" of the MLB fatigue load spectrum. This means tracing fatigue crack growth back to small crack lengths by identifying crack growth markings due to severe simulated flights.
- Estimate the fatigue "initiation" life and fatigue crack growth behaviour for this largest window frame crack.
- Estimate the fatigue "initiation" life and fatigue crack growth behaviour for (a) the largest crack in any of the GLARE aluminium layers, and (b) the largest crack in the GLARE aluminium layers at the same fastener hole as the largest window frame crack
- Compare the fatigue "initiation" and fatigue crack growth behaviour for the GLARE skin and aluminium window frame.
- Provide data to verify and possibly improve fatigue crack growth models for GLARE.

8.3 Practical details

The NDI-indicated fastener holes in the GLARE skin and aluminium window frames were opened up using the procedure described already in subsection **5.2** and illustrated by figure 4.

The selected GLARE fracture surfaces were exposed to a low-temperature oxygen plasma for 30 – 45 minutes in an Emitech K1050X Plasma Asher. The adhesive was completely degraded, enabling easy separation of the aluminium and glass fibre layers. However, the sample temperatures remained below about 60 - 80°C, which meant that the aluminium fatigue fracture surfaces were undamaged.

Fractography was done using a Field Emission Gun Scanning Electron Microscope (FEG-SEM). The FEG-SEM's high resolution is essential for studying fatigue at low growth rates.

8.4 Fractographic "readability" of the MLB fatigue load spectrum

The largest crack in the aluminium window frames was at fastener hole D19 in window area C65 – C66, see tables 5 and 7. FEG-SEM fractography showed that fatigue fracture was a mixture of faceted and mainly continuum-mode areas. The continuum-mode areas contained evident crack front markings due to the peak loads in severe simulated flights.

Figure 9 gives an example of identifying the severe simulated flights, notably the severest flight types A, B and C. The crack front markings from these flights were mostly sufficient for tracing fatigue crack growth back to small crack lengths. However, the fainter crack front markings from D type flights helped in checking the numbering of B and C type flights. In general, the fractographic "readability" was excellent.

8.5 Fractographic analysis of the largest window frame crack

The excellent fractographic "readability" of the largest window frame crack enabled tracing crack growth back from the end of the MLB test to a crack length a ≤ 0.2mm. This was necessary to obtain the following information:

- Fatigue crack growth curves
  - a *versus* N
  - da/dN *versus* a*
- An estimate of fatigue "initiation" life.

where N is the number of simulated flights, da/dN is the fatigue crack growth rate, and a* is the mean crack length for the crack growth interval used to calculate da/dN.

Figures 10a and 10b show the curves of a *versus* N and da/dN *versus* a*, respectively. Both figures show the effects of severe simulated flights, pointed out explicitly in figure 10b. Most of these effects appeared to be transient.

However, beginning at a crack length of 0.6mm there was a significant and persistent retardation of fatigue crack growth. This persistent retardation could be due to termination of the "short crack effect". This effect is well known, and is generally attributed to a lack of fatigue crack closure in cracks smaller than about 0.5mm. Thus once the crack in the window frame grew beyond about 0.5mm, closure-induced retardation effects of peak loads in severe simulated flights would have become possible.

Back-extrapolation of the a *versus* N curve in figure 10a suggests that the fatigue "initiation" life was zero, and that there was an initial crack size of about 0.06mm.

In fact, the crack initiated from a fretting scar due to fastener movement against the bore of the fastener hole (Wanhill *et al*. 2006)[6]. This explains the effectively zero fatigue "initiation" life and also the indication of an initial crack size, which was most probably due to the fretting scar.

8.6 Fractographic analysis of the GLARE cracks

The largest "readable" crack in any of the GLARE aluminium layers was at fastener hole B4 in window area C65 – C66. This crack was 0.91mm long, slightly less than a_{max} , see table 4. The largest crack in the GLARE aluminium layers at the same fastener hole as the largest window frame crack was at fastener hole D19 in window area C65 – C66, see table 7. This crack was only 0.42mm long.

Preliminary examination of these cracks showed that the initial 0.2mm was obscured by debris and sealant. This made fractographic analysis of the smaller crack impractical – there was simply too little fatigue fracture surface available.
As before, the largest "readable" crack was analysed to obtain the following information:

- Fatigue crack growth curves
  - a *versus* N
  - da/dN *versus* a*
- An estimate of fatigue "initiation" life.

where N is the number of simulated flights, da/dN is the fatigue crack growth rate, and a* is the mean crack length for the crack growth interval used to calculate da/dN.
Figures 11a and 11b present the crack growth curves. The data are limited, but sufficient to show that the "plateau" crack growth rates were about 50% of those in the aluminium window frame.

Back-extrapolation of the a *versus* N curve in figure 11a is unfeasible, owing to the limited data. Hence an estimate of the fatigue "initiation" life is not possible.

9 Concluding discussion

9.1 NDI verification

The NDI and low-magnification fractography for a GLARE window area from the MegaLiner Barrel (MLB) test demonstrated that the NLR's teardown NDI capability is excellent, and that most cracks in GLARE will be detected during teardown. Specifically, the mean POD curve for GLARE skin cracks showed that at the 90% probability + 50% confidence level the detectable crack length is 0.25mm.

9.2 Low-magnification fractography

Besides NDI verification, the low-magnification fractography established the patterns of cracking in the GLARE skin, and also the window frames.
Most of the cracks in the GLARE skin were in the fastener hole bores rather than the countersinks. The smaller cracks showed that they began from one or both corners of an aluminium layer, whether in the bores or countersinks.

The preference for GLARE cracking in the fastener hole bores is possibly due to local secondary bending. The window frame cracks make this possibility likely, since these cracks were all corner cracks with maximum dimensions along the fastener hole bores.

9.3 Detailed fractography

Firstly, the detailed fractography demonstrated the fractographic "readability" of the MLB fatigue load spectrum. The "readability" and traceability were excellent for the largest window frame crack, but less so for the largest crack in the GLARE aluminium layers. There are two reasons for this: (a) the crack growth rates for the aluminium layer crack were much lower than those for the window frame crack, making resolution of the crack front markings more difficult; and (b) debris and sealant obscured a considerable part of the initial growth of the aluminium layer crack.

The largest window frame crack was traced back to 0.15mm. Back-extrapolation suggested that the fatigue 'initiation" life was zero, and that there was an initial crack size of about 0.06mm. These results are best explained by the fact that the crack initiated at a fretting scar. Fretting is known to cause very early crack initiation (Waterhouse 1981)[7], and the fretting scar could act as an apparent initial crack size.

The largest "readable" GLARE aluminium layer crack could not be traced back to less than 0.45mm, owing to ever more closely-spaced crack markers, making them impossible to resolve. This, and the limited data, made it unfeasible to estimate a fatigue "initiation" life. Nevertheless, it was evident that this crack grew significantly slower than the largest window frame crack.

9.4 Verification of GLARE crack growth models

One of the main objectives of the present investigation was to provide data to verify and possibly improve current fatigue crack growth models for GLARE. However, all the GLARE aluminium layer cracks were much too small to contribute to this objective: see, for example, the models proposed by Toi (1995)[8], Wu and Guo (1999)[9], and De Koning (2001)[10].

On the positive side, these teardown results are a demonstration of the high fatigue damage tolerance capability of the MLB GLARE skin. This conclusion is reinforced by the fact that the applied fatigue load spectrum was set at a level high enough to obtain fatigue damage during the MLB test.

References

1. M. Wagner, Fatigue Loads Program for MegaLiner Barrel, Report No. 00L020K4700I02, March 2001, Airbus Deutschland GmbH, Hamburg, Germany.
2. S. I. Vukelich, C.L. Petrin, Jr., and C. Annis, Jr., A Recommended Methodology for Quantifying NDE/NDI Based on Aircraft Engine Experience, AGARD Lecture Series 190, April 1993, Advisory Group for Aerospace Research and Development, Neuilly sur Seine, France.
3. A. Fahr, D.S. Forsyth and M. Bullock, A Comparison of Probability of Detection (POD) Data Determined Using Different Statistical Methods, Report LTR-ST-1947, December 1993, National Research Council of Canada, Ottawa, Canada.
4. F.P. Grooteman, Personal Communication, 2005, National Aerospace Laboratory NLR, Amsterdam, the Netherlands.
5. R.J.H. Wanhill, T. Hattenberg and W. van der Hoeven, A Practical Investigation of Aircraft Pressure Cabin MSD Fatigue and Corrosion, Report NLR-CR-2001-356, June 2001, National Aerospace Laboratory NLR, Amsterdam, the Netherlands.
6. R.J.H. Wanhill, T. Hattenberg, D.J. Platenkamp and A.F. Bosch, MegaLiner Barrel Teardown Programme. Part 2: Fractographic Examination and Analysis of Fatigue Cracks for the F4 Window Panel, NLR Contract Report NLR-CR-2005-666, April 2006, National Aerospace Laboratory NLR, Amsterdam, the Netherlands.
7. R.B. Waterhouse, Theories of Fretting Processes, *Fretting Fatigue*, (Editor R.B. Waterhouse), Applied Science Publishers Ltd, London, UK, 1981, pp. 203-219.
8. Y. Toi, An Empirical Crack Growth Model for Fiber / Metal Laminates, *ICAF 95*, *Estimation, Enhancement and Control of Aircraft Fatigue Performance*, (Editors J.M. Grandage and G.S. Jost), Vol. II, Engineering Materials Advisory Services Ltd, Warley, UK, 1995, pp. 899-909.
9. X.-R. Wu and Y.-J. Guo, Fatigue Life Prediction of Fiber Reinforced Metal Laminates under Constant and Variable Amplitude Loading, *Fatigue '99*, *Proceedings of the 7th International Fatigue Congress*, Vol. 3, Higher Education Press, Beijing, China, 1999, pp. 1637-1646.
10. A.U. de Koning, Analysis of the Fatigue Crack Growth Behaviour of "Through the Thickness" Cracks in Fibre Metal Laminates (FML's), NLR Contract Report NLR-CR-2000-575, November 2001, National Aerospace Laboratory NLR, Amsterdam, the Netherlands.

Figure 1 GLARE window area cut from the MLB

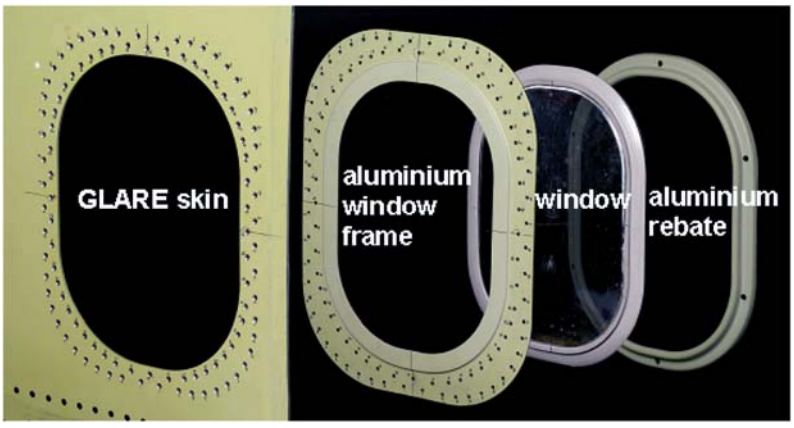

Figure 2 Example of a disassembled window

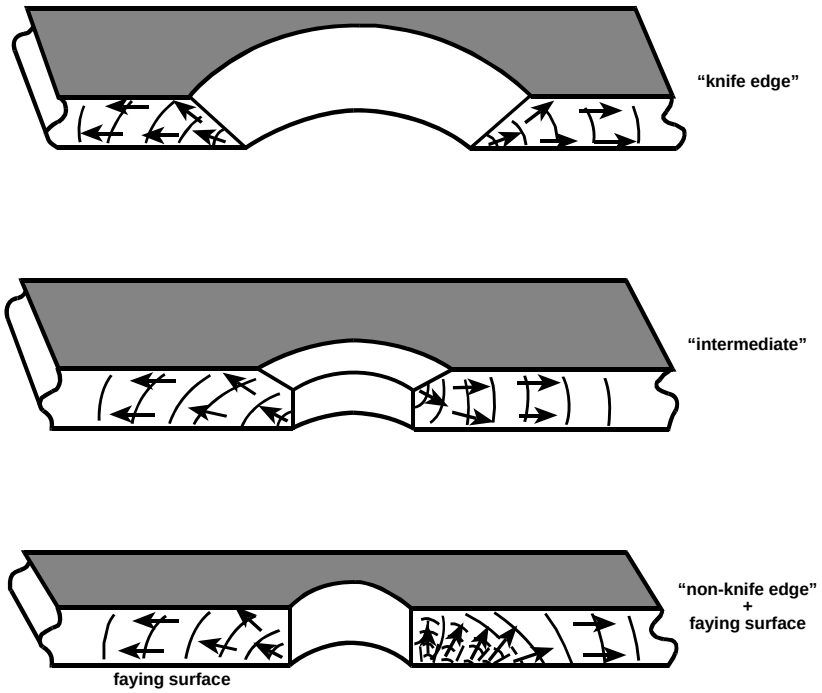

Figure 3 Schematic of possible fatigue initiation and growth sites in GLARE : crack length, a , is along the aluminium layers

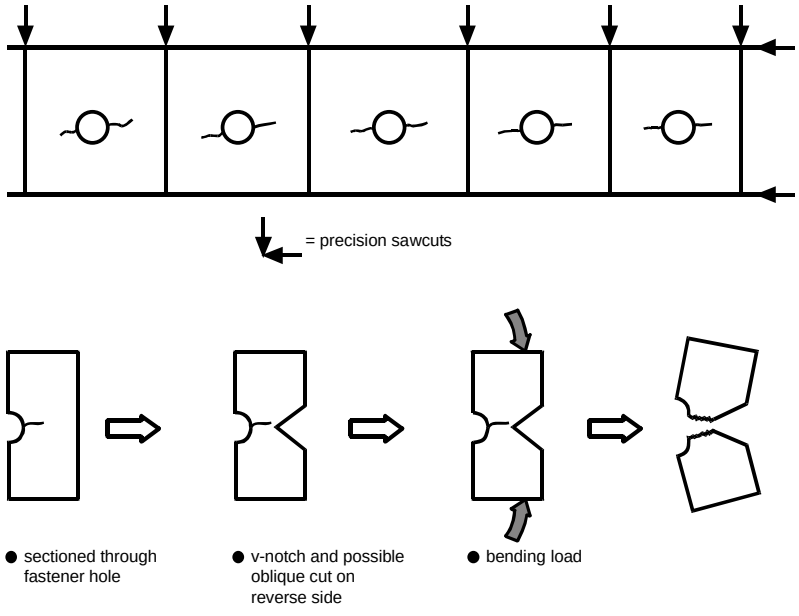

Figure 4 Procedure for opening GLARE cracks

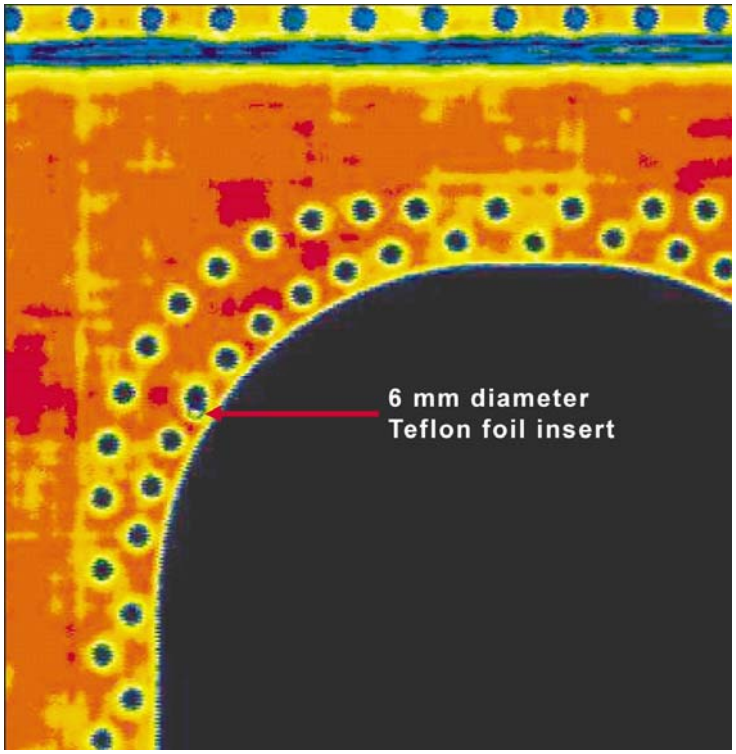

Figure 5 C-scan attenuation detection of the insert

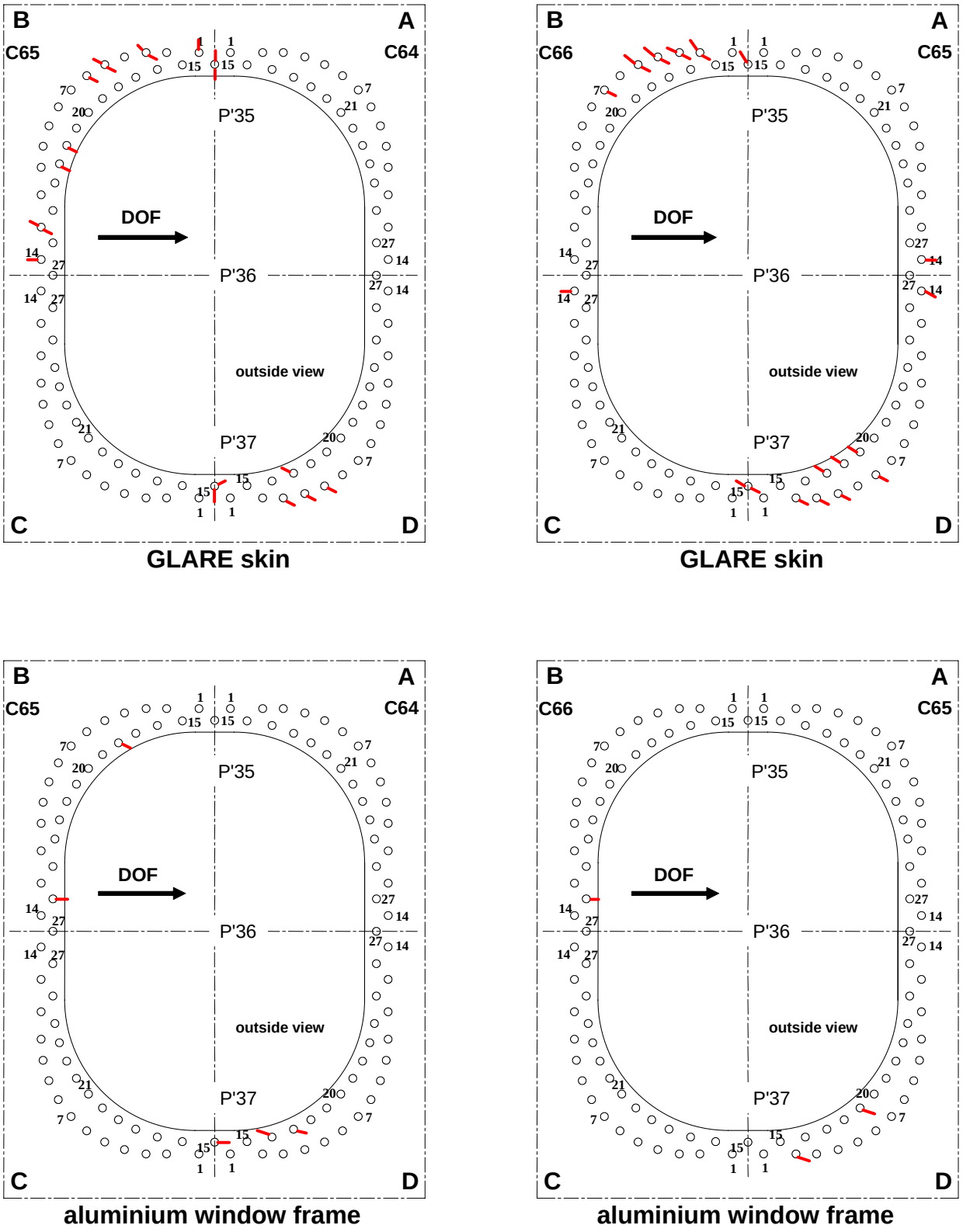

Figure 6 Overviews of the crack indications from eddy current rotor inspections of the fastener hole bores of the fully disassembled GLARE skin and aluminium window frames: ***DOF*** *= Direction Of (simulated)*

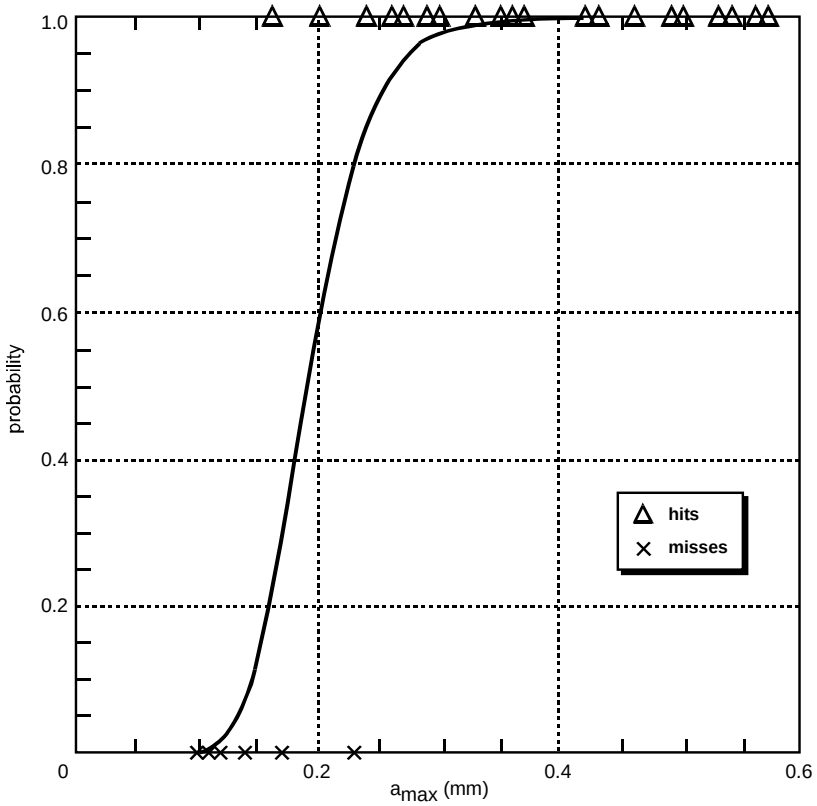

Figure 7 Mean POD curve for GLARE skin cracks

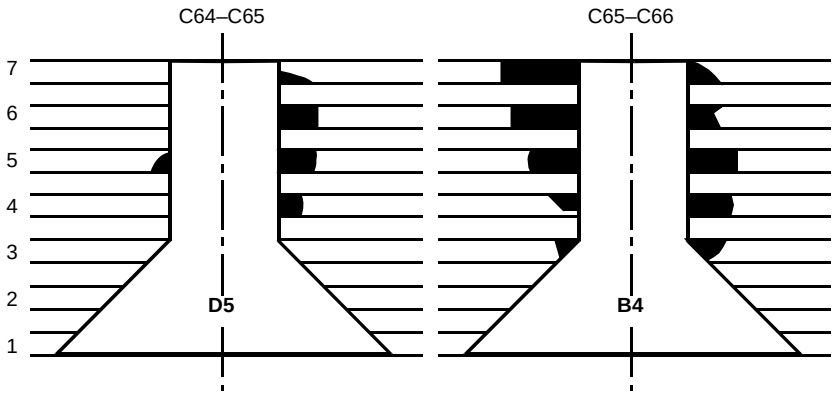

Figure 8 Examples of GLARE cracking patterns

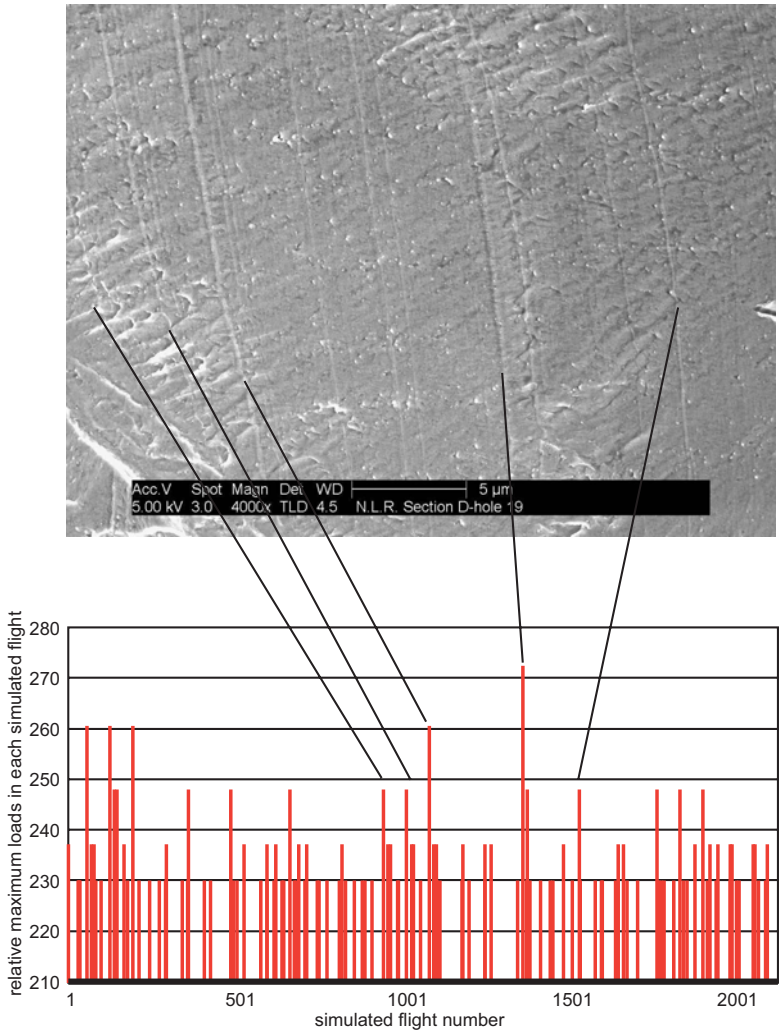

Figure 9 Example of fractographic identification of severe simulated flights from crack front markings due to peak loads

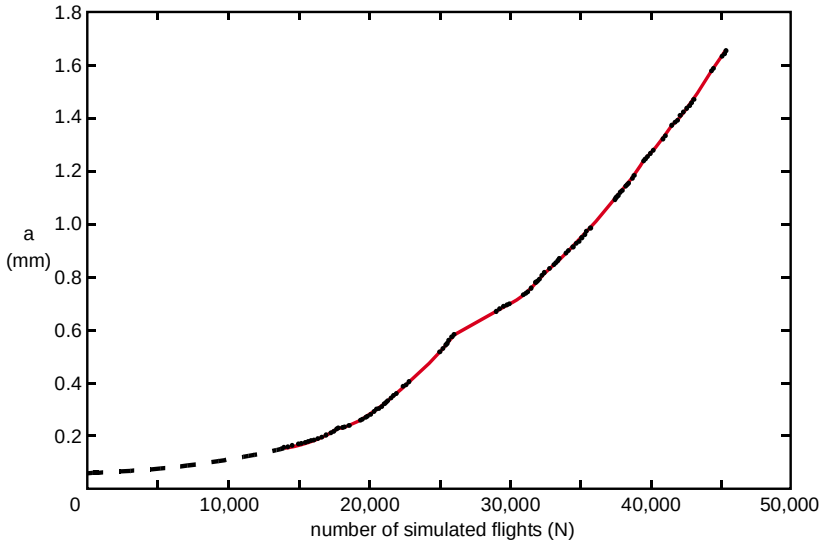

(a) Crack length *versus* number of simulated flights

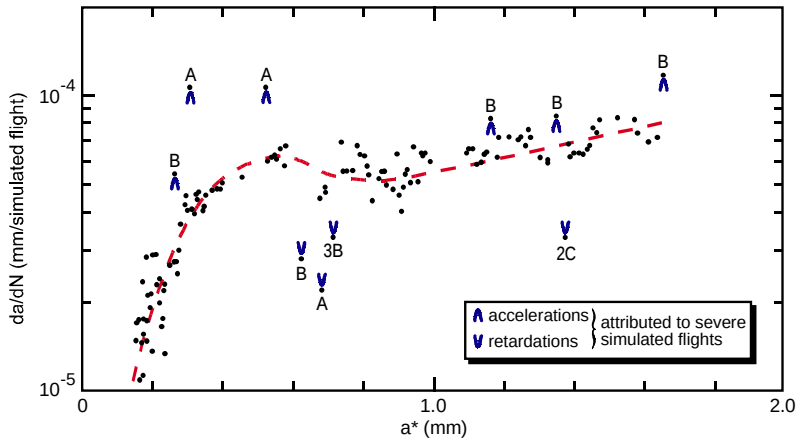

(b) Crack growth rates *versus* mean crack lengths

Figure 10 Crack growth curves for the largest fastener hole crack in either of the window frames.The material was die forged aluminium alloy 7175-T73

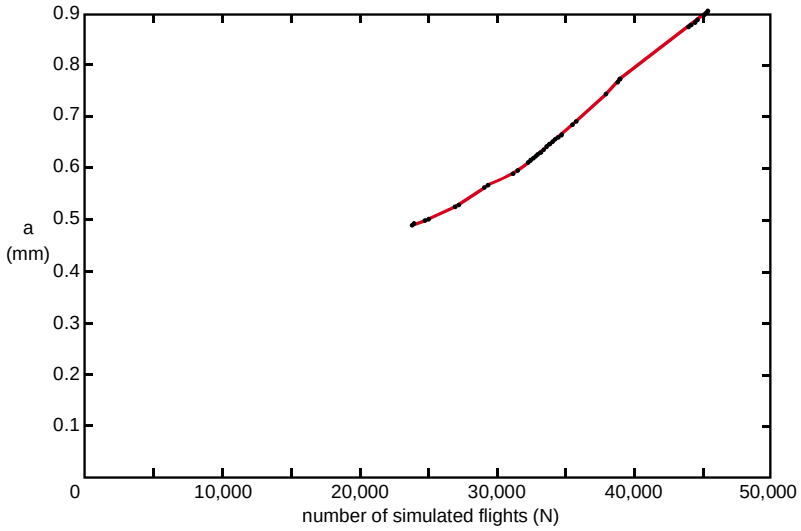

(a) Crack length *versus* number of simulated flights

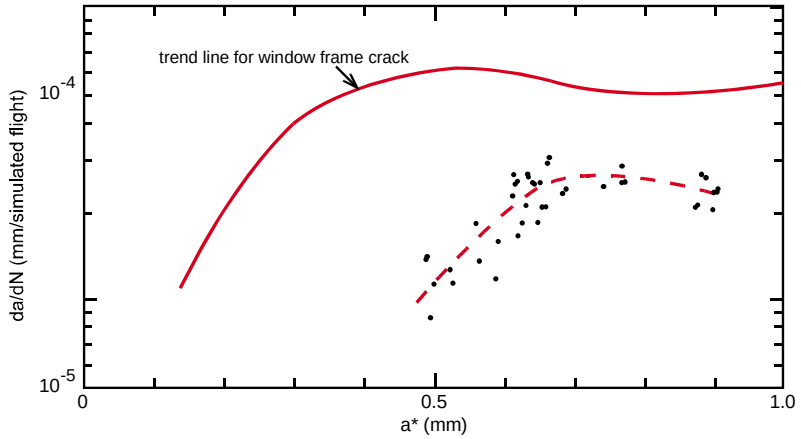

(b) Crack growth rates *versus* mean crack lengths

Figure 11 Crack growth curves for the largest "readable" fastener hole crack in an aluminium layer of the GLARE skin. The material was 0.3mm 2024-T3 sheet